

# Electron Transfer Rates in Bridged Molecular Systems: A Phenomenological Approach to Relaxation

William B. Davis,<sup>\*,†</sup> Michael R. Wasielewski,<sup>†,‡</sup> and Mark A. Ratner<sup>†</sup>

Department of Chemistry, Northwestern University, 2145 N. Sheridan Road, Evanston, Illinois 60208-3113, and Chemistry Division, Argonne National Laboratory, Argonne, Illinois 60439-4831

Vladimiro Mujica

Escuela de Química Facultad de Ciencias, Universidad Central de Venezuela, Apartado 47102, Caracas 1020A, Venezuela

Abraham Nitzan

School of Chemistry, Tel Aviv University, Tel Aviv 69978, Israel

Received: March 13, 1997; In Final Form: May 29, 1997<sup>⊗</sup>

A model for bridge-assisted, long-range electron transfer in a molecule interacting with a dissipative external bath is presented. The effects of the system–bath interaction are included phenomenologically in the evolution of the system density matrix as energy dephasings on the bridge sites. When the bridge dephasings are small, the steady state ET rate in this model is found to be the sum of two competing terms; the first is a McConnell-type rate arising from direct tunneling from donor to acceptor, and the second is a dephasing-dependent, length-independent scattering channel through the bridge sites. In the limit of large dephasings, an incoherent channel dominates the dynamics and leads to ET rates that can become only weakly dependent ( $k_{\text{ET}} \propto 1/N$ ) on the number of bridge sites in the system, for multisite bridges.

## I. Introduction

In both synthetic and biological systems, nonadiabatic long-range electron transfer is one of the most actively pursued areas of contemporary chemistry.<sup>1–18</sup> In biological molecules such as cytochromes, hemoglobins, DNA, and docked proteins long-range electron transfer has been investigated over time scales running down to the femtosecond regime, and it is generally found that, in the nonadiabatic regime, the rate of electron transfer decays roughly exponentially with distance between donor and acceptor sites.<sup>7,11</sup> Synthetic molecules have been prepared by a number of research groups, to investigate specifically the rate of nonadiabatic intramolecular electron transfer as the relative geometries and energetics of the donor and acceptor moieties vary and, particularly, as the distance between donor and acceptor, linked together by rigid bridges, is varied.<sup>5</sup> For example, Chart 1 shows several molecules prepared in our group for the study of such electron transfer phenomena.<sup>19–21</sup>

In the extensive literature on distance-dependent electron transfer in molecular systems, we are aware of no systematic observation of any change with length other than the exponential relationship

$$k_{\text{ET}} = A(T) \exp(-\beta R_{\text{DA}}) \quad (1)$$

Here  $k_{\text{ET}}$ ,  $A(T)$ ,  $\beta$ , and  $R_{\text{DA}}$  are respectively the observed electron transfer rate; a prefactor that includes effects due to reorganization energies and temperature, vibrations, Franck–Condon factors, and the other important rate-determining phenomena; an inverse decay length that generally depends on the energies; and the distance between the centers of the donor and acceptor

sites.<sup>1,4</sup> Indeed, this relationship is so widespread that much of the current discussion often centers only on the magnitude of the  $\beta$  constant and how it varies with chemical structures and energetics.<sup>4,22</sup>

A derivation of the exponential relationship of eq 1 can be presented in several ways; in a chemical context, the first important derivation was given by McConnell,<sup>23</sup> who used perturbation theory to discuss superexchange mixing of donor and acceptor sites by intervening orbitals. McConnell's results have been rederived and generalized many times.<sup>6,10,12,17,24</sup> Exponential behavior also occurs, of course, for simple tunneling through a barrier,<sup>25</sup> and that derivation has also been used to justify, explain, and discuss exponential decay in long-range electron transfer.<sup>26</sup> More elaborate models, using semiempirical electronic structural computation, ab-initio electronic structure theories, pathway pictures, and simple overlap arguments, have all been used to justify exponential dependence.<sup>27</sup>

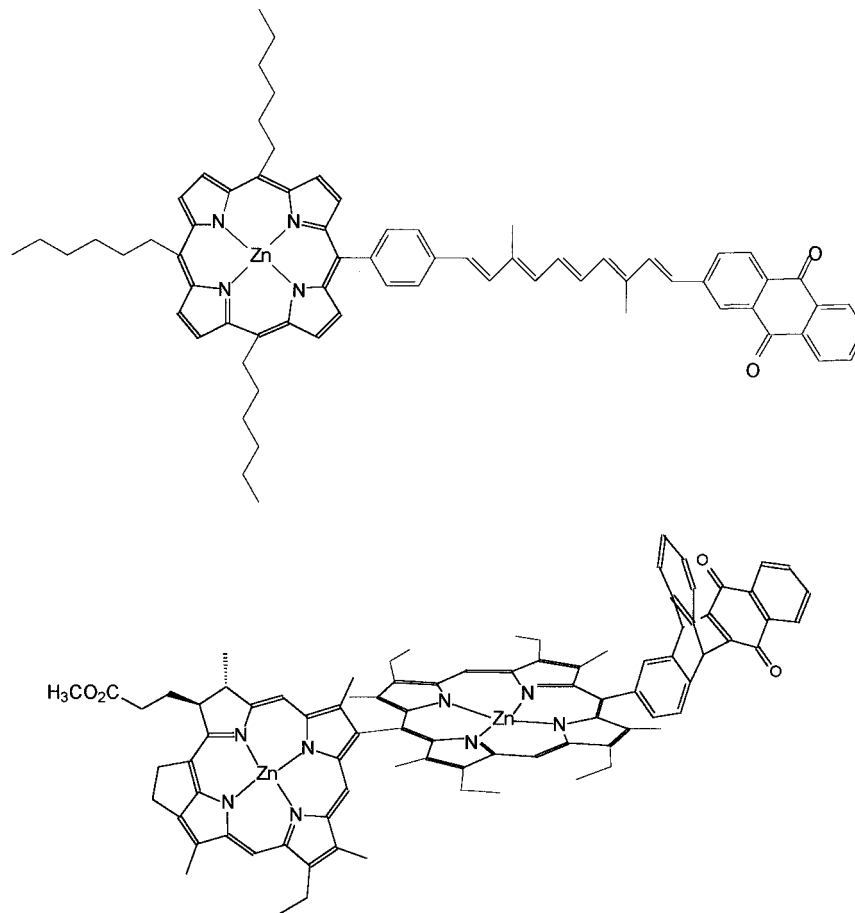
There have been a few reports in the literature in which the exponential dependence is very shallow,<sup>28–31</sup> i.e.  $\beta$  sufficiently small that the exponential decay is unimportant, and some in which other functional forms are obtained.<sup>32</sup> In conjugated conducting polymers, for example, exponential decay of conductance with distance is generally not observed. Rather, these materials really do behave according to Ohm's law: that is, the electrons seem to be localized in the bridging structure between the termini of the extended conductive network, and conductance is determined by scattering processes that are generally inelastic and can correspond to motion of defect carriers such as solitons or polarons.<sup>4,33–37</sup> Quantitatively, an understanding of the difference between the exponential decay of eq 1 and ohmic behavior can be determined starting with the McConnell result:<sup>23</sup> when the energy gap separating donor and acceptor species from the electronic states of the bridge becomes sufficiently small, states will mix, electron/vibration coupling or electron/electron scattering or electron/defect scat-

<sup>†</sup> Northwestern University.

<sup>‡</sup> Argonne National Laboratory.

<sup>⊗</sup> Abstract published in *Advance ACS Abstracts*, August 1, 1997.

## CHART 1



tering will be strong enough that electron localization on the bridge can occur, and exponential decay should no longer be expected. Similar behaviors have been seen in theoretical studies of a number of systems, including particularly molecular wire structures: here the injection energies can be taken as arbitrarily close to the electronic states of the band, and exponential decay is replaced by either power law decay or, in the absence of scattering mechanisms, no decay at all.<sup>22,38-41</sup>

In the analogous situation of electron transfer through tunneling barriers in semiconductor devices, it has been suggested that incoherent processes arising from inelastic scatterings can result in the transformation from exponential decay to ohmic behavior, with the current dominated by inelastic processes and decreasing only slowly, as the inverse of the length of the wire.<sup>42</sup> Recently, similar results have been obtained in theoretical work on long-range electron transfer.<sup>43-45</sup> For example, Friesner and his collaborators used the Redfield<sup>46-49</sup> approach to quantum dynamics in the presence of a dissipative environment to show that, under appropriate temperature and coupling conditions, long-range exponential decay is replaced by a much weaker process, which when displayed in logarithmic coordinates, appears to exhibit essentially no distance decay in the limit of long chains.

In the present work we offer a simpler approach to the same problem. Our technique is based upon supplementing the Liouville equation describing the time evolution of the system's density matrix with phenomenological terms describing thermal relaxation, and the simplification is achieved by focusing on the steady state solution of the resulting equation. A similar approach was used before<sup>50</sup> to describe the transition from coherent Raman scattering to incoherent fluorescence in molecular spectroscopy. It should be emphasized that this approach

can be made rigorous by including a microscopic derivation of the relaxation rate coefficients;<sup>51</sup> however, here we focus on the phenomenological approach. Furthermore, in the present work we deal with only one possible relaxation mechanism: dephasing of the bridge levels. A phenomenological relaxation parameter that describes the dephasing of the electron as it passes through the bridging unit is added to the evolution equations of the nondiagonal elements of the density matrix associated with the bridge sites. This dephasing process arises from the interaction of the electronic system with other bridge and solvent motions. Introduction of these terms shows quite clearly that, in the simple limit of nearest neighbor coupling, there are two independently contributing mechanisms for long-range electron transfer: with large gap energies and weak mixings, and for short chains with relatively small dephasing strengths, the McConnell behavior (superexchange-type coupling, exponential decay with distance) is recovered. For longer chains, higher temperatures, stronger dephasings, smaller gaps, or stronger electronic mixings, long-range behavior decays much more slowly, approaching the ohmic regime, in which the rate is simply given by

$$k_{\text{ET}} = \text{const}/R_{\text{DA}} \quad (2)$$

This very weak dependence on length, corresponding to true wire behavior, is expected in the regime in which incoherent motion, determined by an inelastic scattering, dominates the rate process.

In the usual semiclassical analysis of electron transfer rates, the rate is expressed in the form

$$k_{\text{ET}} = \frac{2\pi}{\hbar} |H_{\text{DA}}|^2 (\text{FCWD}) \quad (3)$$

In eq 3,  $H_{\text{DA}}$  is the electronic matrix element coupling the donor and acceptor and FCWD is a Franck–Condon-weighted density of states.<sup>26</sup> In these semiclassical treatments, distance dependence arises from both  $H_{\text{DA}}$  and FCWD, with the dominant contribution provided by the former.<sup>1</sup> Since semiclassical treatments are developed using perturbation theory, there are implicit assumptions made about the relative magnitudes of certain system parameters. For instance, it is assumed that the couplings between the electronic states are much less than the reorganization energies. Our analysis differs because we make a direct calculation of the electron transfer rate without relying on perturbation theory. Therefore, a direct comparison between our results and those of, for instance, the high-temperature Jortner result<sup>26</sup> is complicated. For example, in our treatment vibronic coupling enters via dephasings, and the inverted regime is not seen.

The phenomenological density matrix theory analysis of the rate process is given in section II. Section III discusses the observed behaviors and rationalizes them in terms of the different contributing processes. Some conclusions are ventured in section IV.

## II. Theory

The Hamiltonian for a quantum mechanical system interacting with a bath can be expressed as

$$\mathbf{H} = \mathbf{H}_S + \mathbf{H}_B + \mathbf{H}_{\text{SB}} \quad (4)$$

where the three terms on the right-hand side of eq 4 are the system, bath, and system–bath Hamiltonians, respectively. In the absence of system–bath coupling, the dynamics of the quantum mechanical system is fully described by the time evolution of either its reduced density matrix<sup>52,53</sup> or the system operators. For the reduced density matrix of a quantum system, the quantum Liouville equation becomes ( $\hbar = 1$ )

$$\dot{\rho} = -i[\mathbf{H}_S, \rho] + \mathbf{L}_D \quad (5)$$

where  $\mathbf{L}_D$  includes the dynamical influences of the last two terms in eq 4.

Instead of utilizing one of the more formal relaxation theories,<sup>54–60</sup> we incorporate the system–bath coupling in a phenomenological way by replacing  $\mathbf{L}_D$  in eq 5 by appropriate relaxation terms. This makes the analysis of the quantum dynamics much simpler by avoiding many of the complications associated with the more rigorous theories, such as concerns about proper separation of the system and bath and nonphysical evolution of the quantum mechanical observables.<sup>52,61,62</sup> A similar phenomenological relaxation theory was applied to elucidate the relation between resonance Raman and resonance fluorescence and serves as guide for including relaxation parameters in the current model.<sup>50</sup> It should be emphasized that the resulting phenomenological equations can be derived as approximations to the rigorous evolution equation (eq 5).

The electron transfer system of interest here consists of an electron donor and acceptor, connected by  $N$  bridge sites. Our system Hamiltonian has the form

$$\mathbf{H}_S = |D\rangle\omega_D\langle D| + |A\rangle\omega_A\langle A| + \sum_{i=1}^N |i\rangle\omega_i\langle i| + [|D\rangle V_{D1}\langle 1| + |N\rangle V_{NA}\langle A| + \sum_{i=1}^{N-1} |i\rangle V_{i,i+1}\langle i+1|] + \text{c.c.} \quad (6)$$

In this formulation, each site has an energy  $\omega_i$  and is coupled in a tight binding fashion to its nearest neighbors by an electronic coupling of magnitude  $V_{i,i+1}$ .

The equations of motion for this quantum system can now be written down using the quantum Liouville equation and incorporating the relaxation parameters of interest. As an example, in the  $N = 2$  system the equations of motion are

$$\begin{aligned} \dot{\rho}_{\text{DD}} &= -2 \text{Im}(V_{\text{1D}}\rho_{\text{D1}}) + C \\ \dot{\rho}_{\text{11}} &= -2 \text{Im}(V_{\text{D1}}\rho_{\text{1D}}) - 2 \text{Im}(V_{\text{21}}\rho_{\text{12}}) \\ \dot{\rho}_{\text{22}} &= -2 \text{Im}(V_{\text{12}}\rho_{\text{21}}) - 2 \text{Im}(V_{\text{A2}}\rho_{\text{2A}}) \\ \dot{\rho}_{\text{AA}} &= -2 \text{Im}(V_{\text{2A}}\rho_{\text{A2}}) - \kappa\rho_{\text{AA}} \\ \dot{\rho}_{\text{D1}} &= iV_{\text{D1}}\rho_{\text{DD}} - i\omega_{\text{D1}}\rho_{\text{D1}} + iV_{\text{21}}\rho_{\text{D2}} - iV_{\text{D1}}\rho_{\text{11}} - \frac{1}{2}\gamma\rho_{\text{D1}} \\ \dot{\rho}_{\text{D2}} &= iV_{\text{12}}\rho_{\text{D1}} - i\omega_{\text{D2}}\rho_{\text{D2}} + iV_{\text{A2}}\rho_{\text{DA}} - iV_{\text{D1}}\rho_{\text{12}} - \frac{1}{2}\gamma\rho_{\text{D2}} \\ \dot{\rho}_{\text{DA}} &= iV_{\text{A2}}\rho_{\text{D2}} - i\omega_{\text{DA}}\rho_{\text{DA}} - iV_{\text{D1}}\rho_{\text{1A}} - \frac{1}{2}\kappa\rho_{\text{DA}} \\ \dot{\rho}_{\text{12}} &= -iV_{\text{1D}}\rho_{\text{D2}} + iV_{\text{12}}\rho_{\text{11}} - i\omega_{\text{12}}\rho_{\text{12}} + iV_{\text{A2}}\rho_{\text{1A}} - iV_{\text{12}}\rho_{\text{22}} - \gamma\rho_{\text{12}} \\ \dot{\rho}_{\text{1A}} &= -iV_{\text{1D}}\rho_{\text{DA}} + iV_{\text{2A}}\rho_{\text{12}} - i\omega_{\text{1A}}\rho_{\text{1A}} - iV_{\text{12}}\rho_{\text{2A}} - \frac{1}{2}\gamma\rho_{\text{1A}} - \frac{1}{2}\kappa\rho_{\text{1A}} \\ \dot{\rho}_{\text{2A}} &= -iV_{\text{21}}\rho_{\text{1A}} + iV_{\text{2A}}\rho_{\text{22}} - i\omega_{\text{2A}}\rho_{\text{2A}} - iV_{\text{2A}}\rho_{\text{AA}} - \frac{1}{2}\gamma\rho_{\text{2A}} - \frac{1}{2}\kappa\rho_{\text{2A}} \quad (7) \end{aligned}$$

with  $\rho_{ij} = \rho_{ji}^*$ ,  $V_{ij} = V_{ji}^*$ , and  $\omega_{ij} = \omega_i - \omega_j$ . Electronic population is injected into the donor site by some unspecified source with a flux given by  $C$ , and the acceptor site is coupled to a population sink inducing a decay with a characteristic rate  $\kappa$ . Thermal dephasing in the bridge appears here in the relaxation (with rate  $\gamma$ ) of all nondiagonal elements of the density matrix associated with the bridge levels. In the language of magnetic resonance,  $\gamma$  corresponds to a  $1/T_2$  processes, and  $\kappa$  corresponds to a  $1/T_1$  process.<sup>63</sup>

In our model, we calculate directly the rate of decay of the initial state rather than a rate constant. The equations of motion (eq 7) can be re-expressed in the matrix form

$$\dot{\rho} = \mathbf{A}\cdot\rho + \mathbf{C} \quad (8)$$

where  $\mathbf{A}$  is the  $(N+2) \times (N+2)$  matrix of coefficients,  $\rho$  is an  $(N+2)^2 \times 1$  vector consisting of the reduced density matrix elements, and  $\mathbf{C}$  is an  $(N+2)^2 \times 1$  vector with the element corresponding to  $\rho_{\text{DD}}$  equal to  $C$  and all others zero. While the equations of motion could be solved numerically to investigate the evolution of the electronic population, we are more interested in the steady state solution for the rate of electron transfer from the donor to acceptor. At steady state, all  $\dot{\rho}_{ij}$  are equal to zero. The electron transfer rate can be calculated as the ratio between the steady state flux through the system,  $\kappa\rho_{\text{AA}}^{\text{SS}} = C$ , and the population of the donor level,  $\rho_{\text{DD}}^{\text{SS}}$ .

$$\text{rate} = \frac{C}{\rho_{\text{DD}}^{\text{SS}}} \quad (9)$$

By utilizing eq 8, the calculation of  $\rho_{DD}^{SS}$  can be performed quickly and efficiently using simple matrix inversion techniques.

### III. Results and Discussion

For simplicity, we have taken  $\omega_D = \omega_A$ , and we have assumed that the bridge is constructed of identical chemical units, so that the bridge site energies become degenerate. Thus, the only site-energy-dependent variable in the system becomes the spacing between the donor and the bridge, which we will simply label as  $\omega$ . We also choose to simplify the model further by setting all electronic couplings equal to a single value,  $V$ . With these assignments, our electron transfer rates will be functions of the four independent parameters  $\omega$ ,  $\gamma$ ,  $V$ , and  $\kappa$ , as well as the number of bridge sites in the system.

It should be emphasized that the bridge dephasing rates  $\gamma$  and the effective electronic couplings between the sites are temperature dependent. This dependence is not displayed explicitly in eq 7. Also, eq 7 neglects the possibility of a thermally activated transmission from the donor to the bridge; that is, it assumes that the corresponding energy gap is much larger than  $K_B T$ .

Extracting the rate, eq 9, from eq 7 or its equivalent is facilitated by the Mathematica package.<sup>64</sup> For  $N = 1$  we get

$$\text{rate} = \left( \frac{1}{4}\gamma^2\kappa^2V^2 + \frac{1}{4}\gamma\kappa^3V^2 + 2\gamma\kappa V^4 + \kappa^2V^4 \right) \left( \frac{1}{8}\gamma^3\kappa^2 + \frac{3}{16}\gamma^2\kappa^3 + \frac{1}{16}\gamma\kappa^4 + \frac{5}{4}\gamma^2\kappa V^2 + \frac{5}{4}\gamma\kappa^2V^2 + \frac{1}{4}\kappa^3V^2 + 2\gamma V^4 + \kappa V^4 + \frac{1}{2}\gamma\kappa^2\omega^2 + \frac{1}{4}\kappa^3\omega^2 \right) \quad (10)$$

While eq 10 may appear daunting at first, when investigated in specific limits of the model parameters it leads to several interesting predictions:

(a) If  $\gamma$  is much smaller than the other three parameters in this model, then those terms of  $O(\gamma^2)$  and higher may be ignored in eq 10.

(b) If in addition  $\omega > \kappa$ ,  $V$ , then eq 10 can be rearranged to

$$\text{rate} = \frac{4V^4}{\kappa\omega^2} + \gamma \left( \frac{V}{\omega} \right)^2 \quad (11)$$

Since the rate is given as a sum, then the overall electron transfer rate is governed by competition between two distinct electron transfer channels. The first part of eq 11 is a McConnell<sup>23</sup> superexchange term, which arises from direct electronic tunneling between the donor and acceptor. In this model, the electronic tunneling rate through a bridge of arbitrary length  $N$  is given by

$$\text{McConnell rate} = \frac{4V^{2N+2}}{\kappa\omega^{2N}} \quad (12)$$

The second term comes from a dephasing-dependent scattering channel, where the bath-induced fluctuations of the bridge site energies cause the electronic population to move from donor to acceptor in a series of short hops through the bridge.

For  $\gamma$  much larger than all other parameters, the three-site rate (eq 10) becomes

$$\text{rate} = \frac{2V^2}{\gamma} \quad (13)$$

Note here that the rate is dependent on the inverse of the dephasing rate. This dependence of the incoherent transfer rate upon the dephasing magnitude in the two different extremes

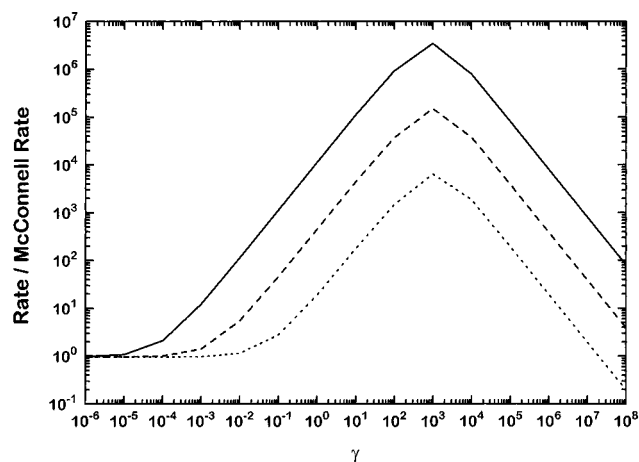


**Figure 1.** Dependence of the ratio between the steady state rate predicted by eq 9 and the rate given by the McConnell term in eq 11 on the system–bath coupling parameter  $\gamma$ . The system variables are given the values  $\omega = 1500 \text{ cm}^{-1}$ ,  $V = 300 \text{ cm}^{-1}$ , and  $\kappa = 400 \text{ cm}^{-1}$ . The three plots correspond to systems with  $N = 6$  (—),  $N = 5$  (---), and  $N = 4$  (···). As  $\gamma$  increases from zero, there is significant enhancement of the electron transfer rate over the McConnell rate in these long bridges due to the introduction of the incoherent scattering channel. For  $\gamma \gg \omega$  the rate decreases as  $1/\gamma$ .

(proportional to  $\gamma$  at small  $\gamma$ , and to  $\gamma^{-1}$  at large  $\gamma$ ) is reminiscent of the dependence of reaction rates on friction in the classical Kramers theory.<sup>65</sup>

The analytical solution for the four-site system was also calculated using Mathematica; however, the full result will not be presented here because of its excessive length. When analyzed in the small- $\gamma$  limit (all terms of  $O(\gamma^2)$  and higher neglected), and  $\omega > \kappa$ ,  $V$ , the analytical four-site rate becomes

$$\text{rate} = \frac{4V^6}{\kappa\omega^4} + \gamma \left( \frac{V}{\omega} \right)^2 \quad (14)$$

Again, in the small- $\gamma$  limit, the transfer rate becomes the sum of a McConnell superexchange rate and a term proportional to  $\gamma$ . In the large- $\gamma$  limit, the electron transfer rate becomes

$$\text{rate} = \frac{V^2}{\gamma} \quad (15)$$

On the basis of this last result, it appears as though the steady state transfer rate in this model goes like

$$\text{rate} = \frac{2V^2}{N\gamma} \quad (16)$$

in the large- $\gamma$  limit. Numerical solution of the steady state equations for arbitrary  $N$  confirm these results. This behavior is ohmic in nature since the rate is inversely proportional to the number of bridge sites (or equivalently the length of the bridge).

Figure 1 displays the effects of  $\gamma$  on the electron transfer rate for a system with  $\omega = 1500 \text{ cm}^{-1}$ ,  $V = 300 \text{ cm}^{-1}$ , and  $\kappa = 400 \text{ cm}^{-1}$ . As  $\gamma$  increases, the overall electron transfer rate becomes enhanced over the McConnell rate, up to a certain value, after which the rate begins to fall off once more. As the number of bridge sites increases, the enhancement of the rate increases, and the onset of the scattering channel dominance begins at smaller values of  $\gamma$ .

The two most sensitive parameters in this theory are  $V$  and  $\omega$ . According to the McConnell picture, the dependence of the effective electronic coupling on  $V$  goes like  $V^{(N+1)}$ , so as the electronic matrix element between the sites increases, then the rate of electron transfer should increase. But, when the system

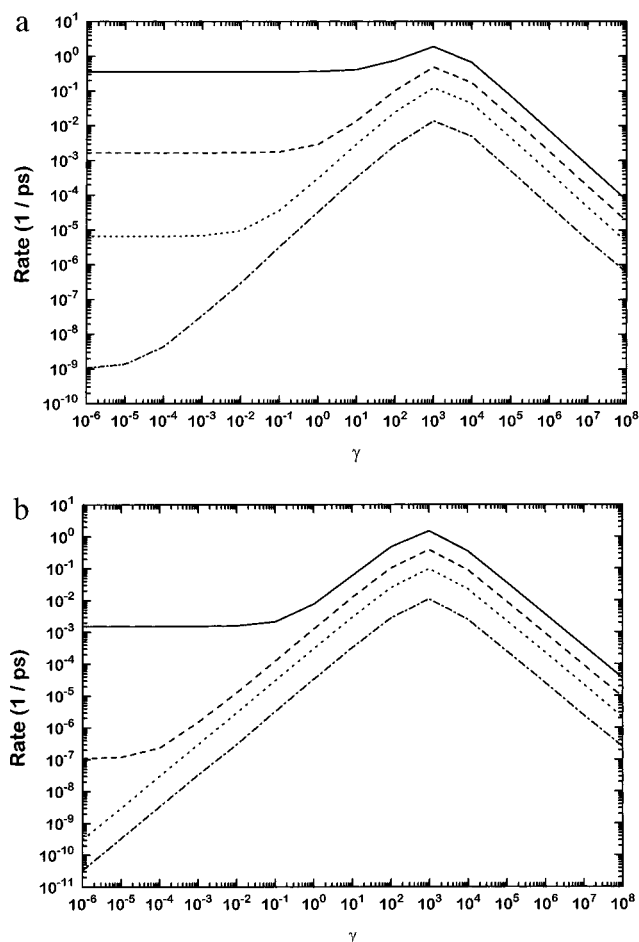


**Figure 2.** Influence of the magnitude of the electronic coupling,  $V$ , on the overall rate of electron transfer in systems with three bridge sites (a) and six bridge sites (b).  $\omega = 1500$  cm<sup>-1</sup>, and  $\kappa = 400$  cm<sup>-1</sup>. In both a and b, the plots correspond to  $V = 600$  cm<sup>-1</sup> (—),  $V = 300$  cm<sup>-1</sup> (---),  $V = 150$  cm<sup>-1</sup> (···), and  $V = 50$  cm<sup>-1</sup> (-·-·). For both bridges, tunneling dominates the rate dynamics up to a  $V$ -dependent critical value of  $\gamma$ , after which the incoherent channel becomes dominant. The higher the value of  $V$ , the higher the overall rate of electron transfer.

is placed in a dissipative bath, competition between the  $\gamma$ -dependent and  $\gamma$ -independent channels, both of which are dependent upon  $V$ , leads to a complex evolution of the rates with increasing electronic coupling. The evolution of the steady state electron transfer rates in this model for the  $N = 3$  and  $N = 6$  cases is presented in Figure 2. In the shorter bridge, even at the smallest electronic coupling considered here, McConnell transport is dominant at smaller  $\gamma$ . As  $V$  increases, the overall rate of electron transfer at each value of  $\gamma$  increases, and the onset of enhancement from the incoherent channel moves toward higher values. In the  $N = 6$  system, at the smallest values of the electronic coupling, the incoherent channel has already become the dominant term governing the evolution of the rates because the tunneling channel is just not efficient enough to dominate the electron transfer process anymore. Note the rate drops with increasing  $\gamma$  in the high- $\gamma$  limit, as predicted by eq 16.

While the rates will generally increase with  $V$ , an opposite effect on the magnitude of the energy gap between the donor and bridge is predicted, so as the sites move farther from resonance, then the rate of electron transfer should decrease. In Figure 3, this  $\omega$  dependence is evident for both the  $N = 3$  and  $N = 6$  systems. For the  $N = 3$  system, the competition between the two channels is dominated by direct tunneling, especially as the sites move close to resonance. In the longer bridge, as

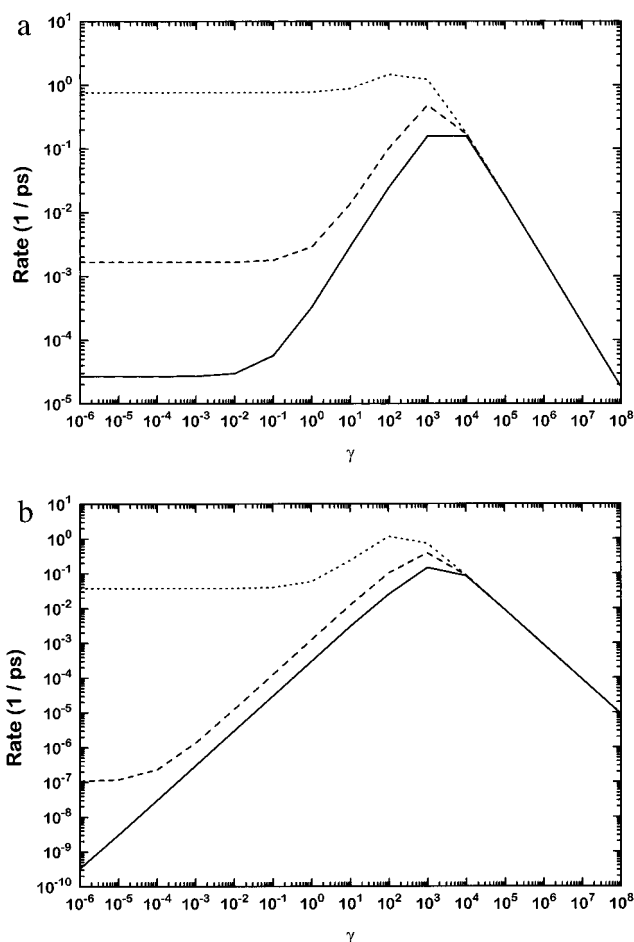


**Figure 3.** Dependence of the electron transfer rates upon the donor-bridge energy gap,  $\omega$ , for both the three-site bridge (a) and the six-site bridge (b).  $V = 300$  cm<sup>-1</sup>, and  $\kappa = 400$  cm<sup>-1</sup>. In both a and b the plots correspond to  $\omega = 3000$  cm<sup>-1</sup> (—),  $\omega = 1500$  cm<sup>-1</sup> (---), and  $\omega = 500$  cm<sup>-1</sup> (···). For both bridges there is an inverse relationship between the rate and  $\omega$  so that as the energy gap increases, then the rate of electron transfer decreases. Also, the farther the donor and bridge sites are from resonance, the stronger the influence of the scattering channel on the rate, especially as the bridge length becomes very long (b,  $\omega = 3000$  cm<sup>-1</sup>). Parts a and b also illustrate the  $\omega$  independence of the transfer rates in the large- $\gamma$  limit.

$\omega$  increases, the scattering channel quickly becomes important in the transfer rates. This is especially apparent in the dynamics at the largest value of the energy gap, where the dependence of the rate on  $\gamma$  is already linear at very small values of the system-bath coupling.

Figure 4 shows the evolution of the electron transfer rate with increasing  $N$ , at three specific values of  $\gamma$ . If the only process available for electron transfer was the superexchange (tunneling) channel, then the electron transfer rate would be expected to fall off exponentially with an increasing number of bridge sites. As soon as the bridge sites couple to the external bath, a second, incoherent, channel opens. In the small- $\gamma$  limit, this channel enhances the transfer rate up to a finite number of bridging sites, after which it will dominate the electron transfer rate. Thus, the electron transfer rate has the behavior displayed in Figure 4 for  $\gamma = 0.001$  cm<sup>-1</sup> and  $\gamma = 1.0$  cm<sup>-1</sup>, where the transfer rate is exponential for short bridges and eventually becomes distance independent for the longer bridges. A rough estimate for the onset of this phenomenon, in the large- $\omega$  limit, comes from setting the rates of the superexchange channel (eq 12) and the scattering channel ( $\gamma(V/\omega)^2$ ) equal to one another and then solving for  $N$ . The result is

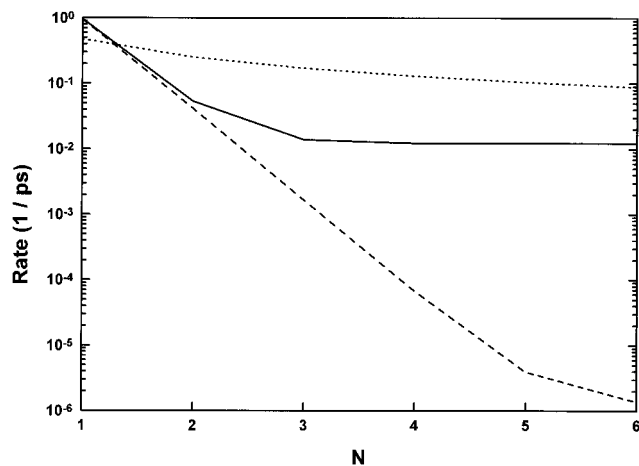


**Figure 4.** Evolution of the electron transfer rates as  $N$ , the number of bridge sites, is increased.  $\omega = 1500 \text{ cm}^{-1}$ ,  $V = 300 \text{ cm}^{-1}$ , and  $\kappa = 400 \text{ cm}^{-1}$ . The plots correspond to systems where the magnitude of the bridge dephasings are  $\gamma = 1.0 \text{ cm}^{-1}$  (—),  $\gamma = 0.001 \text{ cm}^{-1}$  (---), and  $\gamma = 10\,000 \text{ cm}^{-1}$  (···). Even for moderate values of the dephasings, the rates are predicted to quickly become nearly distance independent.

$$N = \frac{\ln[\kappa\gamma/4\omega^2]}{2 \ln[V/\omega]} \quad (17)$$

Hence, the onset of length independence comes at a larger number of sites as  $V$  increases, but at smaller bridge lengths for increasing  $\omega$ ,  $\gamma$ , and  $\kappa$ . Equation 17 predicts that the onset of apparent length independence should occur at a value of  $N = 3$  for  $\gamma = 1.0 \text{ cm}^{-1}$ , and  $N = 5$  for  $\gamma = 0.001 \text{ cm}^{-1}$ . Both predictions are in agreement with the plots of Figure 4. In the limit of large  $\gamma$ , the nearly distance-independent inelastic scattering channel (ohmic behavior) completely dominates the overall rate of electron transfer. The plot for the rate vs  $N$  for the  $\gamma = 10\,000 \text{ cm}^{-1}$  case illustrates the  $k_{\text{ET}} \sim 1/N$  dependence of the electron transfer rates in this regime.

In order to further understand the dynamics of this model in the three transfer regimes (McConnell, distance independent, ohmic), the site populations for the  $N = 4$  system are displayed in Figure 5. The sites are numbered such that the donor is site 1, and site 6 is the electron acceptor. In the McConnell superexchange limit ( $\gamma = 0.0001 \text{ cm}^{-1}$ ), the electronic population is predominately localized on the donor site and falls off rapidly through the bridge. This is as expected, since the bridge sites should act as virtual states in which the electronic population never physically localizes as it traverses the system from donor to acceptor. In the ohmic limit ( $\gamma = 100\,000 \text{ cm}^{-1}$ ), the electronic population on the donor and the four bridge sites are all comparable. In this limit, the electronic dephasings of the bridge sites are so strong that the bridge sites effectively become isoenergetic with the donor, and population will localize on them as it moves between donor and acceptor. For this set of parameters, when  $\gamma = 10 \text{ cm}^{-1}$ , the system is in the regime where  $\gamma(V/\omega)^2$  dominates the McConnell rate, and the steady state rates are distance independent. Here, the donor site population is not quite as dominant as it was in the superexchange limit, and the bridge sites become equivalent with respect to electronic population.

While the weak dependence on distance in the incoherent transfer case seems reasonable, the magnitude of  $\gamma$  at which the onset occurs depends on the details of the model. The frequency-independent dephasing rate  $\gamma$  added to the Liouville equation corresponds to a Lorentzian line shape of the bridge site energies. Equivalently, the relaxation arises from a bath correlation function which is instantaneous ( $\delta$ -correlated).

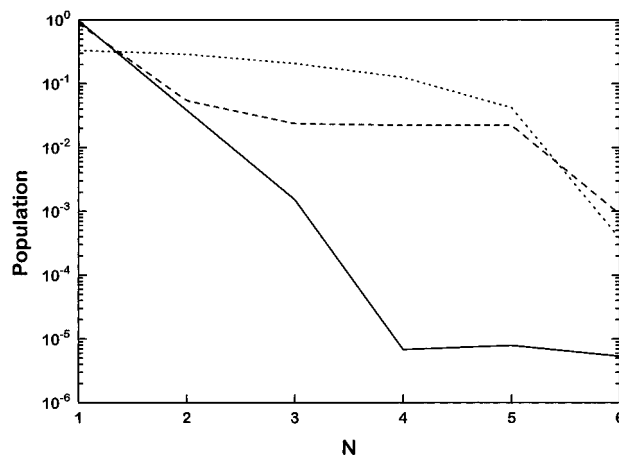


**Figure 5.** Electronic population on each site in the  $N = 4$  system. The donor is labeled as site 1 and the acceptor as site 6.  $C = 1.0 \text{ cm}^{-1}$ ,  $\omega = 1500 \text{ cm}^{-1}$ ,  $V = 300 \text{ cm}^{-1}$ , and  $\kappa = 400 \text{ cm}^{-1}$ . The three values of  $\gamma$ ,  $0.0001 \text{ cm}^{-1}$  (—),  $10 \text{ cm}^{-1}$  (---), and  $100\,000 \text{ cm}^{-1}$  (···), correspond to the system being in the McConnell, distance independent, and ohmic regimes, respectively.

While this form for a bath correlation function is appropriate for its long time behavior, it fails to take into account the time reversal symmetry of correlation functions on short time scales, which would lead to a Gaussian line shape<sup>66</sup> and to a slower onset of flat behavior in Figure 4.

#### IV. Conclusions

Using a phenomenological treatment of the interaction of a quantum mechanical system with an external bath, we have developed a model for long-range electron transfer that displays many of the features seen previously in treatments carried out using the more rigorous Redfield theory.<sup>43,44</sup> In the weak dephasing limit, the two important independent channels for electron transfer, the tunneling and the inelastic scattering, fall readily out of the steady state analytical solutions to the equations of motion. In different limits of the ratio of the magnitude of the electronic coupling to the donor–bridge energy gap, one channel will become dominate over the other. In particular, as the ratio  $V/\omega$  becomes larger, the tunneling rate will dominate the transfer dynamics. Conversely, as  $V/\omega$  decreases, the energy dephasings of the bridge sites begin to play a larger role in determining the electron transfer rates. Since the tunneling rate depends on the number of bridge sites in the system, as the number of bridge sites increases, the scattering rate will begin to dominate at larger values of  $V/\omega$ . In the limit of large coupling, the system is in an ohmic regime where the distance dependence of the electron transfer rates scales as  $1/N$ , and the magnitude of the rate depends on the inverse of the coupling strength.

Perhaps the most intriguing result from this theory is the prediction that even with modest dephasing rates, the electron transfer rates become distance independent. In the absence of system–bath coupling, the simplest McConnell superexchange theory predicts that electron transfer rates will fall off exponentially with increasing bridge length. As soon as the quantum system comes in contact with an external bath, then an effectively distance-independent incoherent channel is turned on, and at some critical bridge length the electronic tunneling rate becomes too small in magnitude to compete effectively. Several experimental studies have shown weak distance dependence of the observed electron transfer rates in these types of donor–bridge–acceptor molecules, including molecules with short-chain oligomers of conjugated organic polymers<sup>67</sup> and

dithiaspiro<sup>68</sup> bridging units. With that said, much more work along these lines is required before any definite conclusion could be reached as to the possible importance of the incoherent mechanism and the breakdown of the exponential decay (rate  $\propto \exp(-\beta N)$ ) in these bridged donor/acceptor systems.

**Acknowledgment.** We are grateful to the USDOE and to the chemistry division of the NSF for support of this research. We also thank the NSF and CONICIT for support through the Joint Venezuela/USA research program. W.B.D. thanks the Link Foundation for fellowship support. A.N. thanks the Israel Ministry of Science for financial support. This work was supported by the Division of Chemical Sciences, Office of Basic Energy Sciences, U.S. Department of Energy, under Contract W-31-109-Eng-38.

## References and Notes

- Marcus, R. A.; Sutin, N. *Biochim. Biophys. Acta* **1985**, *811*, 265–322.
- Newton, M. D. *Chem. Rev.* **1991**, *91*, 767–792. Cave, R. C.; Newton, M. D. In *Molecular Electronics*; Jortner, J., Ratner, M. A., Eds.; Blackwells: London, 1997. Cave, R.; Newton, M. D. *Chem. Phys. Lett.* **1996**, *249*, 15–19.
- Mikkelsen, K. V.; Ratner, M. A. *Chem. Rev.* **1987**, *87*, 113.
- Barbara, P. F.; Meyer, T. J.; Ratner, M. A. *J. Phys. Chem.* **1996**, *100*, 13148.
- Wasielowski, M. R. *Chem. Rev.* **1992**, *92*, 435.
- Evenson, J. W.; Karplus, M. *J. Chem. Phys.* **1992**, *96*, 5272–5278; *Science* **1993**, *262*, 1247–1249.
- Moser, C. C.; Keske, J. M.; Warncke, K.; Farid, R. S.; Dutton, P. L. *Nature* **1992**, *355*, 796–802. Farid, R. S.; Moser, C. C.; Dutton, P. L. *Curr. Opin. Struct. Biol.* **1993**, *3*, 225–233.
- Bjerrum, M. J.; Casimiro, D. R.; Chang, I.-J.; DiBilio, A. J.; Gray, H. B.; Hill, M. G.; Langen, R.; Mines, G. A.; Skov, L. K.; Winkler, J. R.; Wuttke, D. S. *J. Bioenerg. Biomembr.* **1995**, *27*, 295–302. Langen, R.; Chang, I.; Germanas, J. P.; Richards, H. J.; Winkler, J. R.; Gray, H. B. *Science* **1995**, *268*, 1733–1735. Casimiro, D. R.; Richards, J. H.; Winkler, J. R.; Gray, H. B. *J. Phys. Chem.* **1993**, *97*, 13073–13077.
- Gehlen, J. N.; Daizadeh, I.; Stuchebrukhov, A. A.; Marcus, R. A. *Inorg. Chim. Acta* **1996**, *243*, 271–282. Stuchebrukhov, A. A. *J. Chem. Phys.* **1996**, *104*, 8424–8432; *Ibid.*, in press. Hsu, C.-P.; Marcus, R. A. *J. Chem. Phys.*, in press.
- Meade, T. J. *Metal Ions in Biological Systems*; Sigel, A., Sigel, H., Eds.; Marcel Dekker, Inc.: New York, 1996; Vol. 33, p 453.
- Ogawa, M. Y.; Moreira, I.; Wishart, J. F.; Isied, S. S. *Chem. Phys.* **1993**, *176*, 589.
- Ratner, M. A. *J. Phys. Chem.* **1990**, *94*, 4877.
- Brun, A. M.; Harriman, A. *J. Am. Chem. Soc.* **1992**, *114*, 3656.
- Closs, G. L.; Miller, J. R. *Science* **1988**, *240*, 440.
- Paulson, B.; Pramod, K.; Eaton, P.; Closs, G. L.; Miller, J. R. *J. Chem. Phys.* **1993**, *97*, 13042.
- Reimers, J. R.; Hush, N. S. *Chem. Phys.* **1990**, *146*, 89.
- Miller, R. J.; Beitz, J. V. *J. Chem. Phys.* **1981**, *74*, 6746.
- Verhoeven, J. W.; Paddon-Row, M. N.; Hush, N. S.; Oevering, H.; Heppener, M. *Pure Appl. Chem.* **1986**, *58*, 1285.
- Wasielowski, M. R.; Johnson, D. G.; Svec, W. A.; Kersey, K. M.; Cragg, D. E.; Minsek, D. W. In *Photochemical Energy Conversion*; Norris, J., Meisel, D., Eds.; 1989; p 135.
- Wasielowski, M. R.; Niemczyk, M. P.; Johnson, D. G.; Svec, W. A.; Minsek, D. W. *Tetrahedron* **1989**, *45*, 4785.
- Johnson, D. G.; Niemczyk, M. P.; Minsek, D. W.; Wiederrecht, G. P.; Svec, W. A.; Gaines, G. L.; Wasielowski, M. R. *J. Am. Chem. Soc.* **1993**, *115*, 5692.
- Joachim, C.; Vinuesa, J. F. *Eur. Phys. Lett.* **1996**, *33*, 635.
- McConnell, H. M. *J. Chem. Phys.* **1961**, *35*, 508–515.
- Beratan, D. N.; Betts, J.; Onuchic, J. N. *Science* **1991**, *252*, 1285.
- For example: Messiah, A. *Quantum Mechanics*; Wiley: New York, 1961; Chapter 3.
- DeVault, *Quantum Mechanical Tunneling in Biological Systems*; Cambridge: Cambridge, 1984.
- Reviews appear, for example, in *Chem. Phys.* **1993**, *176* (2, 3); in *J. Photochem. Photobiol.* **1994**, *82* (1–3); in *J. Phys. Chem.* **1993**, *97* (50).
- Murphy, C. J.; Arkin, M. R.; Jenkins, Y.; Ghatlia, N. D.; Bossmann, S.; Turro, N. J.; Barton, J. K. *Science* **1993**, *262*, 1025.
- Murphy, C. J.; Arkin, M. R.; Ghatlia, N. D.; Bossmann, S.; Turro, N. J.; Barton, J. K. *Proc. Natl. Acad. Sci. U.S.A.* **1994**, *91*, 5315.
- Arkin, M. R.; Stemp, E. D. A.; Holmlin, R. E.; Barton, J. K.; Hörmann, A.; Olson, E. J. C.; Barbara, P. F. *Science* **1996**, *273*, 475.
- Arkin, M. R.; Stemp, E. D. A.; Turro, C.; Turro, N. J.; Barton, J. K. *J. Am. Chem. Soc.* **1996**, *118*, 2267.
- Hush, N. S. *Coord. Chem. Rev.* **1985**, *64*, 135.
- Tsukamoto, J. *Adv. Phys.* **1992**, *41*, 509.
- Cornil, J.; Beljonne, D.; Bredás, J. L. *J. Chem. Phys.* **1995**, *103*, 842.
- Gregorius, H.; Heitz, W.; Müllen, K. *Adv. Mater.* **1993**, *5*, 279.
- Andre, J.-M.; Delhalle, J.; Bredás, J. L. *Quantum Chemistry Aided Design of Organic Polymers*; World Scientific: Singapore, 1991.
- Bredás, J. L.; Silbey, R., Eds. *Conjugated Polymers*; Kluwer: Dordrecht, 1991.
- Kemp, M.; Mujica, V.; Ratner, M. A. *J. Chem. Phys.* **1994**, *101*, 5172.
- Kemp, M.; Mujica, V.; Ratner, M. A. *J. Chem. Phys.* **1994**, *101*, 6849, 6856.
- Mujica, V.; Kemp, M.; Roitberg, A.; Ratner, M. A. *J. Chem. Phys.* **1996**, *104*, 7296.
- Samanta, M. P.; Tian, W.; Datta, S.; Henderson, J. I.; Kubiak, C. P. *Phys. Rev.* **1996**, *B53*, R7626.
- Neofotistos, G.; Lake, R.; Datta, S. *Phys. Rev.* **1991**, *B43*, 2442.
- Felts, A. K.; Pollard, W. T.; Friesner, R. A. *J. Phys. Chem.* **1995**, *99*, 2929.
- Pollard, W. T.; Felts, A. K.; Friesner, R. A. *Adv. Chem. Phys.* **1996**, *93*, 77.
- Skourtis, S. S.; Mukamel, S. *Chem. Phys.* **1995**, *197*, 367–388.
- Redfield, A. G. *IBM J. Res. Dev.* **1957**, *1*, 19. *Ibid. Adv. Magn. Reson.* **1965**, *1*, 1.
- Wertheimer, R.; Silbey, R. *Chem. Phys. Lett.* **1980**, *75*, 243.
- Jean, J. M.; Friesner, R. A.; Fleming, G. R. *J. Chem. Phys.* **1992**, *96*, 5827. Pollard, W. T.; Friesner, R. A. *J. Chem. Phys.* **1994**, *100*, 5054.
- Jean, J. M.; Fleming, G. R. *J. Chem. Phys.* **1995**, *103*, 2092. Jean, J. M. *J. Chem. Phys.* **1996**, *104*, 5638.
- Weitz, D. A.; Garoff, S.; Gersten, J. I.; Nitzan, A. *J. Chem. Phys.* **1983**, *78*, 5324.
- Nitzan, A. *Chem. Phys.* **1979**, *41*, 163.
- Fano, U. *Rev. Mod. Phys.* **1957**, *29*, 74.
- Blum, K. *Density Matrix Theory and Applications*; Plenum Press: New York, 1981.
- Gorini, V.; Koszkowski, A.; Sudarshan, E. C. G. *J. Math. Phys.* **1976**, *17*, 821.
- Lindblad, G. *Commun. Math. Phys.* **1976**, *48*, 119.
- Alicki, R.; Landi, K. *Quantum Dynamical Semigroups and Applications*; Springer Verlag: Berlin, 1987.
- Kosloff, R.; Rice, S. A. *J. Chem. Phys.* **1980**, *72*, 4591.
- Kosloff, R.; Ratner, M. A. *J. Chem. Phys.* **1984**, *80*, 2352.
- Geva, E.; Kosloff, R. *Phys. Rev. E* **1994**, *49*, 3903.
- Kosloff, R.; Ratner, M. A.; Davis, W. B. *J. Chem. Phys.* **1997**, *106*, 7036.
- Suarez, A.; Silbey, R.; Oppenheim, I. *J. Chem. Phys.* **1992**, *97*, 5101.
- Pechukas, P. *Phys. Rev. Lett.* **1994**, *73*, 1060.
- Oxtoby, D. W. *Adv. Chem. Phys.* **1981**, *47*, 487.
- Wolfram, S. *The Mathematica Book*; Wolfram Media/Cambridge University Press: Cambridge, 1996.
- Kramers, H. A. *Physica* **1940**, *4*, 284.
- Schatz, G. C.; Ratner, M. A. *Quantum Mechanics in Chemistry*; Prentice Hall: Englewood Cliffs, NJ, 1993.
- Helms, A.; Heiler, D.; McLendon, G. *J. Am. Chem. Soc.* **1992**, *114*, 6227.
- Stein, C. A.; Lewis, N. A.; Seitz, G. *J. Am. Chem. Soc.* **1982**, *104*, 2596.